Journal of Reproduction and Development, Vol. 66, No 5, 2020

—Original Article—

Expression and possible roles of extracellular signal-related kinases 1-2 (ERK1-2) in mouse primordial germ cell development

Maria SORRENTI[1)*], Francesca Gioia KLINGER[1)*], Saveria IONA[1)], Valerio ROSSI[1)], Serena MARCOZZI[1)] and Massimo DE FELICI[1)]

[1)]*Department of Biomedicine and Prevention, Section of Histology and Embryology, University of Rome "Tor Vergata", Rome 00173, Italy*

Abstract. In the present work, we described the expression and activity of extracellular signal-related kinases 1-2 (ERK1-2) in mouse primordial germ cells (PGCs) from 8.5–14.5 days post coitum (dpc) and investigated whether these kinases play a role in regulating the various processes of PGC development. Using immunofluorescence and immunoblotting to detect the active phosphorylated form of ERK1-2 (p-ERK1-2), we found that the kinases were present in most proliferating 8.5–10.5 dpc PGCs, low in 11.5 dpc PGCs, and progressively increasing between 12.5–14.5 dpc both in female and male PGCs. *In vitro* culture experiments showed that inhibiting activation of ERK1-2 with the MEK-specific inhibitor U0126 significantly reduced the growth of 8.5 dpc PGCs in culture but had little effect on 11.5–12.5 dpc PGCs. Moreover, we found that the inhibitor did not affect the adhesion of 11.5 dpc PGCs, but it significantly reduced their motility features onto a cell monolayer. Further, while the ability of female PGCs to begin meiosis was not significantly affected by U0126, their progression through meiotic prophase I was slowed down. Notably, the activity of ERK1-2 was necessary for maintaining the correct expression of oocyte-specific genes crucial for germ cells survival and the formation of primordial follicles.

Key words: Extracellular signal-regulated kinases (ERKs), Gene expression, Meiosis, Oogenesis, Primordial germ cells

(**J. Reprod. Dev. 66:** 399–409, 2020)

Three main mitogen-activated protein kinase (MAPK) families have been described in mammalian cells: the extracellular signal-regulated kinase (ERK1-2-5), the Jun NH_2-terminal kinase (JNK), and the p38 kinase. MAPKs are involved in the control of many fundamental cellular processes, including proliferation, survival, differentiation, apoptosis, motility, and metabolism. Of the three MAPK pathways, the ERK pathway is the best defined. Briefly, many receptors induce the activation of Ras, a small GTPase that binds to and recruits Raf kinases to the cell membrane for subsequent activation. Activated Raf kinases are the point of entry into a three-tiered kinase cascade in which Raf phosphorylates and activates map-erk kinase (MEK). MEK subsequently phosphorylates and activates ERKs, which have substrates in the nucleus, cytosol, membranes, and cytoskeleton compartments.

It is known that ERKs play an essential role at many levels of mammalian gametogenesis but particularly in the process of meiosis and oocyte activation upon fertilization [1, 2]. Studies performed primarily in mice have shown that after meiotic I resumption in the oocytes, the ERK pathway is required for maintaining the chromatin condensed during the two meiotic divisions and to avoid a second round of DNA duplication. Moreover, ERK activity is involved in the regulation of microtubule organization and meiotic spindle assembly. Eventually, ERK activation is essential for the maintenance of metaphase II arrest before fertilization while inactivation is a prerequisite for pronuclear formation after fertilization or parthenogenetic activation.

MAPKs have been reported to be involved in processes of early gametogenesis when the germ cell lineage precursors, primordial germ cells (PGCs), are formed. PGCs arise extragonadaly and migrate to the presumptive gonadal ridges (GRs), where they differentiate into oogonia/oocytes or prospermatogonia in the developing ovaries and testes, respectively (for a review, see [3]). In the mouse embryo, Aubin and colleagues [4] showed that MAPK and BMP signaling converge on the SMAD1 transcription factor to regulate PGC specification. Shortly thereafter, another transcription factor PRDM14 appears to promote the germline fate and naïve pluripotency by repressing fibroblast growth factor (FGF) signaling and related ERK activity [5]. In 8.5 dpc mouse PGCs, MEK/MAPK-dependent mammalian target of rapamycin (mTOR) signaling activated by the tyrosine-protein kinase KIT and favoring *in vitro* proliferation has been reported [6]. In slices of 9.5–10.5 dpc mouse embryos, about 50% of PGCs showed cytoplasmic staining for p-ERK1-2, which is likely dependent on FGF signaling and involved in sustaining PGC survival and migration toward the GRs [7]. At these stages, the expression of MEK5, an activator of ERK5 and MKK4 that is dependent on the transcriptional repressor RET, has been also reported to prevent PGC apoptosis [8]. After analyzing sections of 11.5 dpc GRs for p-ERK1-2, Chen *et al*. [9] observed active kinases primarily in the cytoplasm and occasionally in the nucleus of about 55% of PGCs.

Received: November 6, 2019
Accepted: April 22, 2020
Advanced Epub: May 16, 2020

Correspondence: M De Felici (e-mail: defelici@uniroma2.it)
* M Sorrenti and FG Klinger contributed equally to the present work.

Such activity was partially dependent on KIT receptors and not critical for PGC survival. On the contrary, PGC survival appeared to rely at least in part on similar KIT-dependent JNK activity. At a later stage of gonad development, RNA sequencing presented strong enrichment in MAPK-related pathways in 13.5 dpc female and male mouse PGCs [10]. Ulu *et al*. [11] showed that *in vitro*, FGF9 increased p-ERK1-2 in 12.5 dpc male PGCs in a concentration-dependent manner, which paralleled the high proliferation and low expression levels of male germ cell differentiation genes (e.g., *Nanos2* and *Dnmt3l*). On the other hand, a low FGF9 concentration was necessary to induce p38 MAPK and high expression of male germ cell differentiation markers. Ewen *et al*. [12] reported that p38 MAPK signaling antagonized entry into meiosis in male PGCs, instead directing the cells toward mitotic quiescence and a spermatogenic fate. Wu *et al*. [13] further demonstrated that p38 MAPK suppressed retinoic acid (RA)-induced meiosis in male PGCs in an independent manner.

A crucial role of ERK1-2 in PGC differentiation of both sexes is evidenced by the fact that using the MEK1-2 inhibitor PD0325091 in combination with a glycogen synthase kinase 3 (GSK3) inhibitor and leukemia inhibiting factor (LIF), both female and male mouse PGCs up to 13.5 dpc can be reprogrammed into pluripotent stem cells termed embryonic germ (EG) cells [14, 15]. Intriguingly but still in line with the results concerning the promoting effect of PRDM14 on germline specification reported above, MEK1-2 inhibition favored the formation of PGC-like cells from embryonic stem (ES) cells in an *in vitro* mesodermal differentiation system [16]. Similarly, the competency of human ES or induced pluripotent stem (iPS) cells to form PGC-like cells was greatly increased by adding a MEK1-2 inhibitor to the culture medium [17, 18].

In the present work, we described the expression and activation of ERK1-2 in mouse PGCs throughout their entire developmental period (8.5–13.5 dpc) and inhibited kinase activity with UO126 in *in vitro* cultures of isolated PGCs or embryonic ovaries. Furthermore, we investigated whether these kinases play a role in regulating various processes of PGC development, including proliferation, migration, entry, and progression into meiosis and oocyte differentiation.

Materials and Methods

Animals and chemicals

CD-1 and transgenic GFP/c-Kit mice (indicated as p18 mice from here onward) [19] were housed and mated under standard laboratory conditions in an environmentally controlled room and treated with humane care according to the Italian and European rules (D.L.116/92; C.E. 609/86; European Directive 2010/63/EU; authorization n°391/2016-PR).

p18 mice were used in order to identify oocytes in whole mount ovaries under a confocal microscope (see below) while CD-1 mice were used in all other experiments and analyses.

U0126 (Sigma-Aldrich, Milan, Italy) was dissolved in dimethyl sulfoxide (DMSO) at 10 mM, aliquoted, and stored at –20°C. All other compounds and reagents were purchased and used as reported in the text.

PGC culture onto STO cell monolayers

PGCs were isolated by enzymatic (2.5 mg/ml trypsin) ethylenediaminetetraacetic acid (EDTA; 1 mM) disaggregation of tissue containing PGCs (8.5 dpc allantois and posterior primitive streak); 10.5 dpc aorta, gonad, and mesonephros (AGM) regions; and 11.5–12.5 dpc GRs of embryos according to the methods described by De Felici [20]. The sex of the 8.5 dpc tissues, 10.5 dpc AGM, and 11.5 dpc GRs was not determined, but from 12.5 dpc onwards, the ovaries and testes were morphologically distinguishable. PGCs were cultured in 96-well Falcon tissue culture onto mitomycin C-inactivated STO cell monolayers (an embryonic mouse fibroblast cell line purchased from ATCC, Manassas, VA, USA) in Dulbecco's Modified Eagle Medium (DMEM; GIBCO/BRL, Milan, Italy) supplemented with 15% fetal calf serum (FCS; GIBCO), 0.1 mM non-essential amino acids, 0.1 mM 2-mercaptotehanol, 2 mM glutamine, and 5 μM forskolin (all from Sigma-Aldrich Milan). The cultures were carried out in a humidified incubator at 37°C and 5% CO_2 in air. Before seeding and after one to two days of culture, PGCs were identified and counted by labeling for alkaline phosphatase (APase) as reported by De Felici [20]. Before seeding, the number of PGCs in the cell suspension was determined by transferring 5–10 μl samples onto poly-l-lysine-coated coverslips (three replicates) followed by APase staining of the attached cells. At the end of culture, all APase-positive cells in each well were counted.

The BrdU incorporation assay was performed on cultured PGCs after 24 h as described by Farini *et al*. [21]. Where indicated, cell viability was estimated using the erythrosine B (Sigma-Aldrich) staining assay as discussed in De Felici and McLaren [22].

PGC adhesion and motility assays

PGC adhesion and motility assays were carried out onto confluent STO cell monolayers after one day of culture as described in Pesce *et al*. [23] and Donovan *et al*. [24] (see also the legend to Fig. 2). Briefly, STO cells were grown to confluence in DMEM supplemented with 10% FCS (GIBCO) in the wells of a Heraeus Flexiperm-Micro 12 (Sigma-Aldrich) tissue chamber attached to a culture Falcon Petri dish (#353003, Falcon; Corning, NY, USA). The number of 11.5 dpc PGCs in the cell suspension was determined in aliquots transferred to poly-l-lysine coated coverslips (three replicates) followed by APase staining (see above). Aliquots of cell suspensions containing 200–300 cells were then seeded onto the cell monolayers, and the Flexiperm chamber was removed after 45–60 min of culture. The dish was then gently washed once with 5 ml of culture medium to remove unattached cells before the remaining cells were fixed with 4% paraformaldehyde for 5 min. The number of adhering germ cells was scored after identification by APase, and PGC adhesion values were calculated as a percentage of the seeded number. In the experiments in which the effect of UO126 was tested, PGCs were preincubated in the culture medium for 40–60 min at 37°C, and the adhesion assay was carried out in the presence of the inhibitor.

Immunofluorescence (IF)

Samples of cell suspensions obtained following enzymatic EDTA (PGC-containing tissues: 8.5 dpc allantois and posterior primitive streak and 10.5 dpc AGM) or EDTA-only (11.5 dpc GRs and 12.5–14.5 dpc gonads) disaggregation were immediately attached to poly-l-lysine-coated slides and fixed in 4% paraformaldehyde for 10 min [20]. The cells were then permeabilized with 0.1% Triton

X-100 and incubated in anti-phospho-p44/42 MAPK (α ERK1-2) [T202/Y204] kinase (p-ERK) rabbit polyclonal antibody (1:250; Cell Signaling, Leiden, The Netherlands) overnight at 4°C. After blocking non-specific signals with phosphate-buffered saline (PBS)-3% bovine serum albumin (BSA) (all from Sigma-Aldrich) for 1 h at room temperature, the samples were incubated with Alexa Fluor 488 Goat anti-Rabbit antibody (1:500; Molecular Probe, Milan) and 5 μg/mL Hoechst (Sigma-Aldrich) for 5 min. In some experiments, to confirm PGC identity before staining with the p-ERK antibody, the cells were stained with TG-1 (recognizing the SSEA-1 antigen) or anti-OCT4 antibodies as reported by Farini *et al*. [21, 25]. At least 5 random fields with approximately 200 cells were scored for each cell preparation (at least 5 for each developmental age were analyzed), and the cells were scored as p-ERK-positive using NIS-Elements software (version 3.21.02; Nikon, Tokyo, Japan) when intensity of the staining higher than the background (determined in samples where only the secondary antibody was used) was observed (see Fig. 1c and 1c′).

Evaluation of meiotic prophase I stages

The 12.5 dpc PGCs were isolated and purified using the MiniMACS (Miltenyi Biotec, Bologna, Italy) immunomagnetic cell sorter method (PGC purity approximately 90%) [26] and cultured onto a Transwell PET membrane filter (Falcon) as reported by Farini *et al*. [21]. The capability of the PGCs to enter into meiosis was evaluated after two days of culture using anti-SCP-3 antibody (ab150292; Abcam, Milan, Italy) as discussed in Farini *et al*. as well as Chuma and Nakatsuji [21, 27]. Scoring was performed as reported in the IF section.

Ovary culture and histological analyses

The 12.5 dpc ovaries with attached mesonephros were dissected from the embryos and washed in the culture medium. For short-term culture (48 h), two or three ovaries freed from the mesonephros were transferred onto a Transwell PET membrane filter (Falcon) and inserted into a 24-well plate Falcon tissue culture dish. The culture medium was α-MEM supplemented with 10% fetal bovine serum (FBS; GIBCO), L-glutamine, penicillin-G, streptomycin, pyruvic acid, and N-acetyl-l-cysteine. For extended culture, the gonads were placed onto Transwell collagen-coated (Transwell-COL) membrane inserts (Costar; Sigma-Aldrich) for a total of 17 days following the method reported by Morohaku *et al*. [28].

For confocal microscope (A1 confocal laser; Nikon) observations, ovaries obtained from p18-GFP mice were fixed in 4% paraformaldehyde and mounted onto slides. Z-stacks were acquired every 2.5 μm or 5 μm. GFP-positive germ cells were counted every six images (corresponding to 15 μm and 30 μm, respectively) to avoid double counting. The images acquired every 2.5 μm were used to count oocytes with a diameter ≤ 20 μm while those acquired every 5 μm were used for oocytes with a diameter > 20 μm. 3D rendering was performed with NIS-Elements software (Nikon) using the alpha-blending algorithm. For conventional histology, ovaries from CD-1 mice were fixed in 0.05 M $NaPO_4$, 1% paraformaldehyde (PFA), and 0.1% glutaraldehyde (all from Sigma-Aldrich). for 4 h at room temperature and processed for paraffin inclusion, sectioning (5 μm thick sections), and hematoxylin-eosin (H&E) staining following standard procedures.

Immunoblotting (western blotting)

The 11.5–13.5 dpc PGCs were isolated and purified using the MiniMACS immunomagnetic cell sorter method from at least 10 GRs or gonads [26]. Where indicated, whole ovaries (at least 10) were also used. First, 5x sodium dodecyl sulfate (SDS; Sigma-Aldrich) sample buffer was added to the tissues before the samples were boiled for 5 min. Proteins (approximately 30 μg) were separated on either 10% or 7.5% SDS-PAGE gels and transferred to PVDF Transfer Membrane Hybond^{Tm}-P (Amersham; Sigma-Aldrich). The membranes were saturated with 5% nonfat dry milk in PBS containing 0.1% Tween 20 for 1 h at room temperature and incubated at 4°C with the following primary antibodies: mouse α-tubulin (1:1000; Sigma-Aldrich), rabbit phospho p44/42 MAPK (α ERK1-2) [T202/Y204] and p44/42 MAPK (1:1000; Cell Signaling), and mouse MVH (1:1000; Abcam). Secondary anti-mouse or α-rabbit IgGs conjugated to horseradish peroxidase (Amersham; Sigma-Aldrich) were incubated with the membranes for 1 h at room temperature following a 1:10000 dilution in TBS/Tween 20. Notably, more proteins on the same blot were detected after the stripping of the membrane using "Restore WB stripping buffer" (Thermo Fisher Scientific, Milan, Italy).

Immunostained bands were detected by the chemiluminescent method (Amersham; Sigma-Aldrich), and densitometry analysis of the bands was performed using TotalLaB image analysis software (Nonlinear Dynamics, Newcastle upon Tyne, UK).

Real-time quantitative reverse transcription polymerase chain reaction (qRT-PCR)

The extraction of total RNA from two or three gonads or oocytes (approximately 50) was performed with Trizol reagent (Ambion, Milan, Italy) according to the manufacturer's instructions. Oocytes were isolated from the 17-day *in vitro*-cultured ovaries by incubation for 30 min in IV collagenase (1 mg/ml) followed by 30 min in 0.01% EDTA at 37°C and then pricked with needles. Released oocytes (diameter > 30 μm) were recovered with a mouth-operated pipette.

RNA was resuspended in 20 μl of RNase- and DNase-free water, and c-DNA synthesis was performed with a PrimeScript RT Reagent Kit with gDNA Eraser (Takara; Sigma-Aldrich). For qRT-PCR, 20–25 ng of cDNA was amplified with the KAPA SYBR FAST qPCR Kit (Kapa Biosystems; Sigma-Aldrich) on the ABI PRISM 7300 Sequence Detection System (Applied Biosystems; Sigma-Aldrich). The reactions were performed in a total volume of 20 μl, which included 2 μl of cDNA, 10 μl of SYBR Green ROX, and 0.5 μM of each primer. Cycling was performed using the following default conditions of the ABI 7300 SDS software version 1.3: 2 min at 95°C followed by 38 cycles of 15 sec at 95°C, 30 sec at 60°C, and 30 sec at 72°C. The means (± SEM) of three experiments were determined for each gene in each group. The primers used are indicated in Table 1.

Statistical analysis

All experiments were replicated at least three times; the number of replicates and gonads used are reported in the Results section and Figures. The means ± SEM were tested for homogeneity of variance and analyzed by ANOVA with Bonferroni's post hoc test using GraphPad Prism software (GraphPad Software, San Diego, CA, USA). The level of significance was set at $P < 0.05$ (*), $P <$

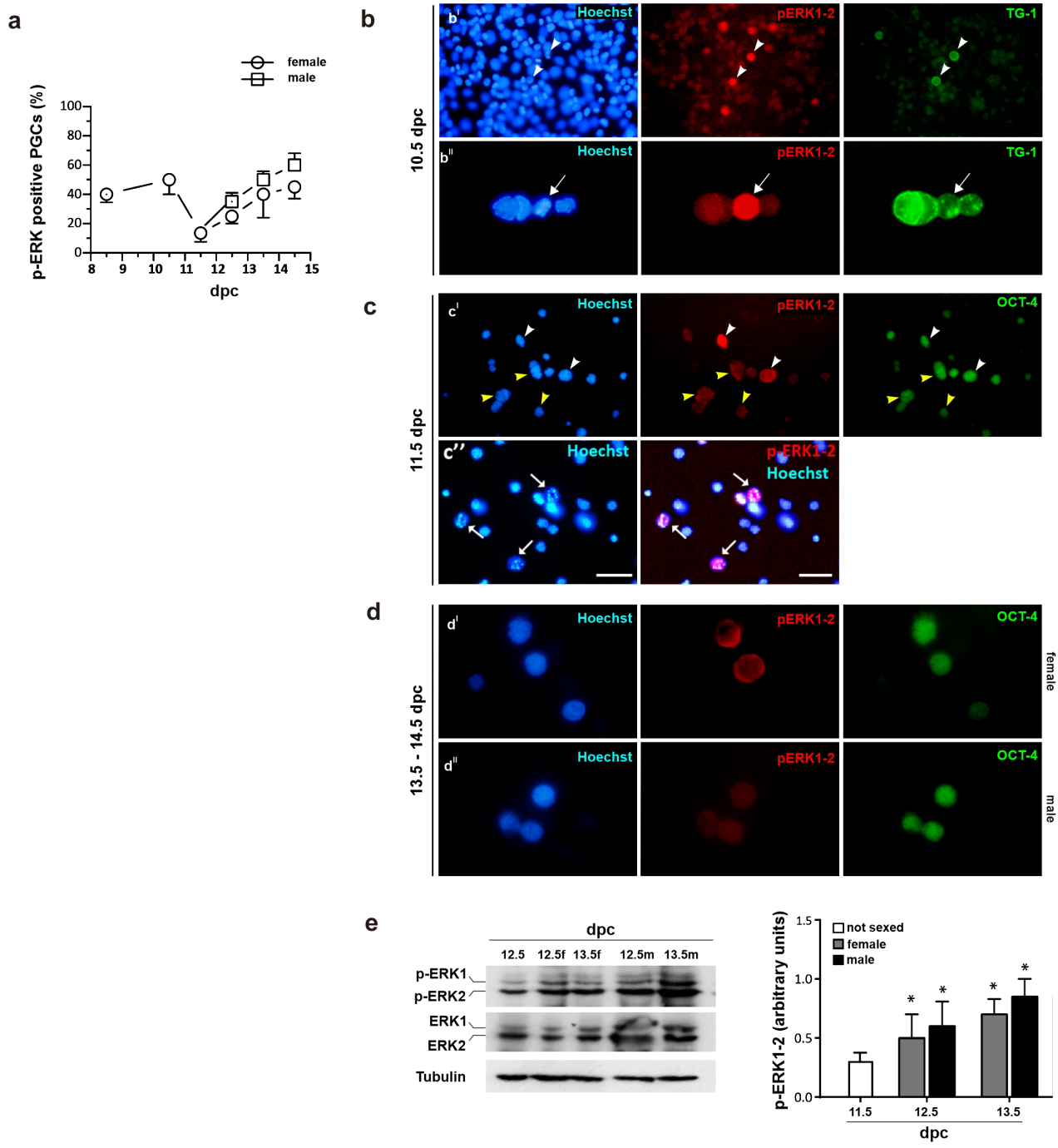

Fig. 1. Expression of p-ERK1-2 during primordial germ cells (PGC) development. a: Percentage of p-ERK1-2-positive PGCs isolated from PGC-containing tissues (8.5 dpc allantois and posterior primitive streak; 10.5 dpc dorsal mesentery and part of gut) or 11.5 dpc gonadal ridges (GRs) and 12.5–14.5 dpc gonads determined following immunofluorescence (IF). The means ± SEM of three experiments are shown. b: 10.5 dpc. b': example of two p-ERK1-2/TG-1-positive PGCs (arrowheads) in a cell population obtained from aorta, gonad, and mesonephros (AGM). Scale bar: 50 µm. b'': cluster of PGCs in which the only p-ERK1-2-positive cell (arrow) shows condensed chromatin. Scale bar: 20 µm. c: 11.5 dpc; c': example of cell population obtained from GRs showing OCT-4-positive PGCs with high (white arrowheads) or moderate (yellow arrowheads) cytoplasmic and nuclear p-ERK1-2 staining. Scale bar: 50 µm. c'': p-ERK1-2-positive PGCs showing condensing chromosomes. Scale bar: 50 µm. d: 13.5–14.5 dpc; d': example of female PGCs showing p-ERK1-2 positivity mainly in the cytoplasm. Scale bar: 20 µm. d'': male PGCs showing p-ERK1-2 positivity both in the cytoplasm and nucleus. Scale bar: 20 µm. e: Representative WB analyses for p-ERK1-2 in PGCs obtained from 11.5 dpc GRs and 12.5–13.5 dpc ovaries (f) as well as testes (m). The graph reports densitometric evaluation of the WB analyses relative to tubulin. The means ± SEM of three experiments are shown. Statistical differences are versus 11.5 dpc GRs. No differences are observed when comparing 12.5 dpc female versus 12.5 dpc male, 13.5 dpc female versus 13.5 dpc male, 12.5 dpc female versus 13.5 dpc female, and 12.5 dpc male versus 13.5 dpc male PGCs.

Table 1. Primers used in the present study

Genes	Sequence 5′–3′	
	Forward	Reverse
Figα	ACAGAGCAGGAAGCCCAGTA	GTCAGAGGGTCTGCCACTGT
Sohlh1	GGGCCAATGAGGATTACAGA	AAGTTTGCAGCAGCCACAG
Sohlh2	TCTCAGCCACATCACAGAGG	GGGGACGCGAGTCTTATACA
Nobox	GGCACTAGTATCGCCTCACC	GGAGAGCTGGAATGAACC
Lhx8	ACACGAGCTGCTACATTAAGGA	CCCAGTCAGTCGAGTGGATG
Mvh	GCTACTCCAGGGAGGCTGATC	TATCCAACATTCGATCAGCTTCA
Foxl2	AAGCCCCCGTACTCGTACGTGGCGCTCATC	GTAGTTGCCCTTCTCGAACATGTC
Gata4	GCCCAAGAACCTGAATAAAT	CGGACACAGTACTGAATGTCT
Gapdh	AACTTTGGCATTGTGGAAGG	CCGTGTTCCTACCCCCAATGTG

0.01 (**), and $P < 0.001$ (***).

Results

Variations in ERK1-2 activity and intracellular localization in 8.5–14.5 dpc PGCs

In the first series of experiments, we used IF to reveal p-ERK1-2 in freshly isolated PGCs from 8.5 to 14 dpc embryos. As reported in Figure 1a, the percent of positive cells was about 50% at 8.5–10.5 dpc, < 10% at 11.5 dpc, and progressively increasing up to 60–70% between 12.5–14.5 dpc without significant sex differences (Figs. 1b–1d). At all stages, most somatic cells did not show consistent staining and therefore were not considered in the other investigations.

In line with these observations, WB analyses of purified PGCs showed a progressively significant p-ERK1-2 increase in PGCs between 11.5 and 13.5 dpc with no significant sex differences (Fig. 1e). In such assays, incubation of PGCs for 30 min in 5 μM U0126 before WB almost completely abolished ERK phosphorylation (not shown).

Inhibition of ERK1-2 activity reduces the proliferation of 8.5 dpc but not 11.5 dpc PGCs

In order to identify PGC functions requiring ERK1-2 activity, we cultured 8.5 and 11.5 dpc PGCs in conditions allowing their proliferation [29, 30] in the presence of 5 or 10 μM U0126. The results reported in Fig. 2a show that while the number of 8.5 dpc PGCs was significantly reduced in the presence of the inhibitor, that of 11.5 dpc PGCs was not affected. The effect of U0126 on 8.5 dpc PGCs was associated with a significant decrease in the number of PGCs in the S-phase of the cell cycle as evaluated by BrdU incorporation (control: 25 ± 3.2% *vs*. 5 μM U0126: 12.5 ± 1.4%; $P < 0.01$), suggesting a reduction in the proliferative capability of such cells. On the other hand, the percentage of cells in the S-phase was not significantly reduced in 11.5 dpc PGCs cultured for 24 h in the presence of the same inhibitor concentration (control: 18.4 ± 1.8% *vs*. 5 μM U0126: 15.2 ± 1.5%).

Motility but not adhesion of PGCs to cell monolayers requires ERK1-2 activity

In a previous work, we found an approximate 30% reduction in PGC migration capability in the presence of 10 μM U0126 using a cell directional migration assay [25]. In the present work, in order to determine which process among many in cell migration might be affected by ERK inhibition in PGCs, we investigated the adhesive behavior and motility morphologies (elongated/polarized or only elongated) [24] of 11.5 dpc PGCs seeded and cultured onto STO cell monolayers with or without U0126. The results in Fig. 2b showed that the number of PGCs adhering to the STO cells at the beginning of culture was not affected by the presence of the inhibitor. However, the frequency of PGCs displaying motility features after 24 h was significantly reduced (Figs. 2c and 2d).

ERK1-2 activity is not required for meiosis entry by female PGCs but necessary for their normal meiotic progression

In mice, the period between 12.5 and 13.5 dpc is crucial for the PGC cell cycle and sex differentiation. In fact, in female embryos, PGCs undergo a transition from mitosis to meiosis and become primary oocytes. The molecular mechanisms controlling such processes are only partly known [21, 27, 31–33]. In order to find a possible correlation between the progressive increase in ERK1-2 activity and the beginning of meiosis, we analyzed the meiotic prophase I stages in cytospreads of 12.5 dpc female PGCs cultured *in vitro* for two days with or without 5–10 μM U0126. While the percentages of germ cells at different meiotic stages in the control ovaries were comparable to those found in ovaries of comparable age *in vivo* (14.5 dpc; unpublished results; pre-leptotene: 21.5 ± 8.7%; leptotene: 34.7 ± 6.5%; zygotene: 43.7 ± 13.0%), we observed that the inhibitor did not interfere with the ability of PGCs to enter meiosis but significantly reduced the frequency of oocytes at the zygotene stage after two days of culture (10 μM U0126: 20.5 ± 7%; Fig. 2e). At this time, no significant differences in the percent of viable germ cells between the control and treated groups (approximately 50–60%) were observed.

Effects of ERK1-2 activity inhibition on the expression of genes involved in oocyte differentiation

Next, we hypothesized that ERK1-2 activity could be required for PGC differentiation into oocytes, a process found to be independent from meiosis but beginning during the same period [34]. In order to substantiate such a possibility, we analyzed the effect of U0126 on the expression of female germ cell-specific genes considered to not

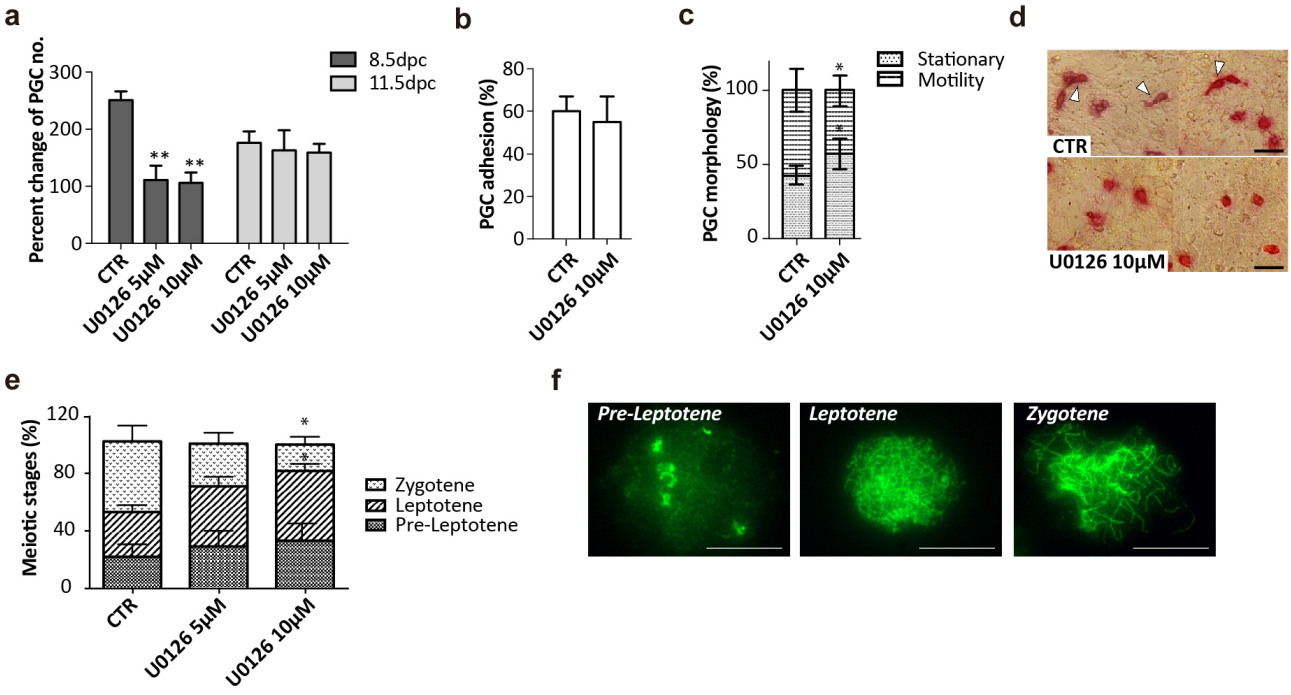

Fig. 2. Effects of inhibition of ERK1-2 activity on primordial germ cells (PGC) growth, adhesion/motility, and meiosis entry/progression. a: Effect of 5 and 10 μM U0126 on the number of 8.5–11.5 dpc PGCs after 24 h of culture. All APase-positive cells present in each replicate (approximately 100–200) were counted and compared to the number of PGCs at the beginning of culture normalized to 100% (see Materials and Methods). The means ± SEM of three experiments each performed in triplicate are shown. b: Effect of 10 μM U0126 on the capability of 11.5 dpc PGCs to adhere to an STO cell monolayer. c and d: Effect of 10 μM U0126 on the motility phenotypes of 11.5 dpc PGCs onto an STO cell monolayer (white arrows in d indicate APase-positive PGCs with motility phenotypes). According to Donovan *et al*. [24], PGCs were considered stationary when closely adherent to the substrate and rounded up or motile when well-spread on the substrate with or without polarization plus features characteristic of motile cells, including filopodia, uroid, and retraction fibers. All APase-positive cells present in each replicate (approximately 200–300) were counted, and the percent of stationary and motile cells were calculated. The means ± SEM of the three experiments each performed in triplicate are shown. Scale bar: 50 μm. e. Percent of meiotic prophase I-stage 12.5 dpc female PGCs after two days of culture. Note a delay in meiotic progression caused by the addition of 5 or 10 μM U0126 to the culture medium. In each group, at least 200 cells in three different experiments were scored. CTR: control. Statistical differences are versus the CTR group. f. Representative PGC cytospreads for SCP-3 immunostaining show the chromosome morphologies of the pre-leptotene, leptotene, and zygotene stages. Scale bar: 5 μm.

be involved in meiosis [35, 36] using *in vitro* cultured ovaries. First, however, we verified if the activation pattern of ERK1-2 observed *in vivo* was maintained in culture. The results of WB analysis confirmed that p-ERK1-2 increased significantly during *in vitro* culture and that ERK activity was almost completely abolished by 5 μM U0126 (Supplementary Fig. 1a: online only).

For oocyte-specific genes, we chose *Figα, Nobox, Lhx8, Sohlh1,* and *Sohlh2* and used RT-PCR for a preliminary evaluation of their respective expression levels in freshly dissected GRs (11.5 dpc) and ovaries [from 12.5 dpc to 1 day post-partum (dpp)] in addition to 12.5 dpc ovaries cultured for 48 h. The resulting expression patterns of these genes are shown in Figs. 3a and 3b. In summary, *in vivo*, none of the genes were expressed in 11.5 dpc GRs, but *Sohlh2* began to be expressed at 12.5 dpc followed by *Sohlh1* and *Figα* at 13.5 dpc as well as *Nobox* and *Lhx8* at 14.5 dpc. Thereafter, the expression of all genes increased with variable patterns. The expression patterns of these genes evaluated in 12.5 dpc ovaries cultured *in vitro* for 48 h essentially reflected the distinct variations described *in vivo* (Supplementary Figs. 1b and 1c).

In order to evaluate whether ERK1-2 activity was required for the expression of the genes mentioned above, 12.5 dpc ovaries were cultured for 48 h with or without 5 μM U0126. The mRNA expression levels of these genes and *Mvh*, which was employed as germ cell-specific housekeeping gene, were quantified by qRT-PCR. As shown in Fig. 3c, the transcript levels of all genes except *Mvh* were significantly reduced in the presence of the inhibitor, particularly those of *Nobox*, *Sohlh2*, and *Sohlh1*. Such decreases were not caused by a reduction in oocyte number since it was not significantly different between the control and treated ovaries (control: 1519 ± 13; U0126: 1532 ± 55; n = 3 ovaries analyzed for each condition). In line with this notion, as reported above, the expression level of the germ cell-specific housekeeping gene *Mvh* remained constant. Similarly, the mRNA levels of *Folx2* and *Gata4* specific to the supporting somatic cells were not affected by U0126.

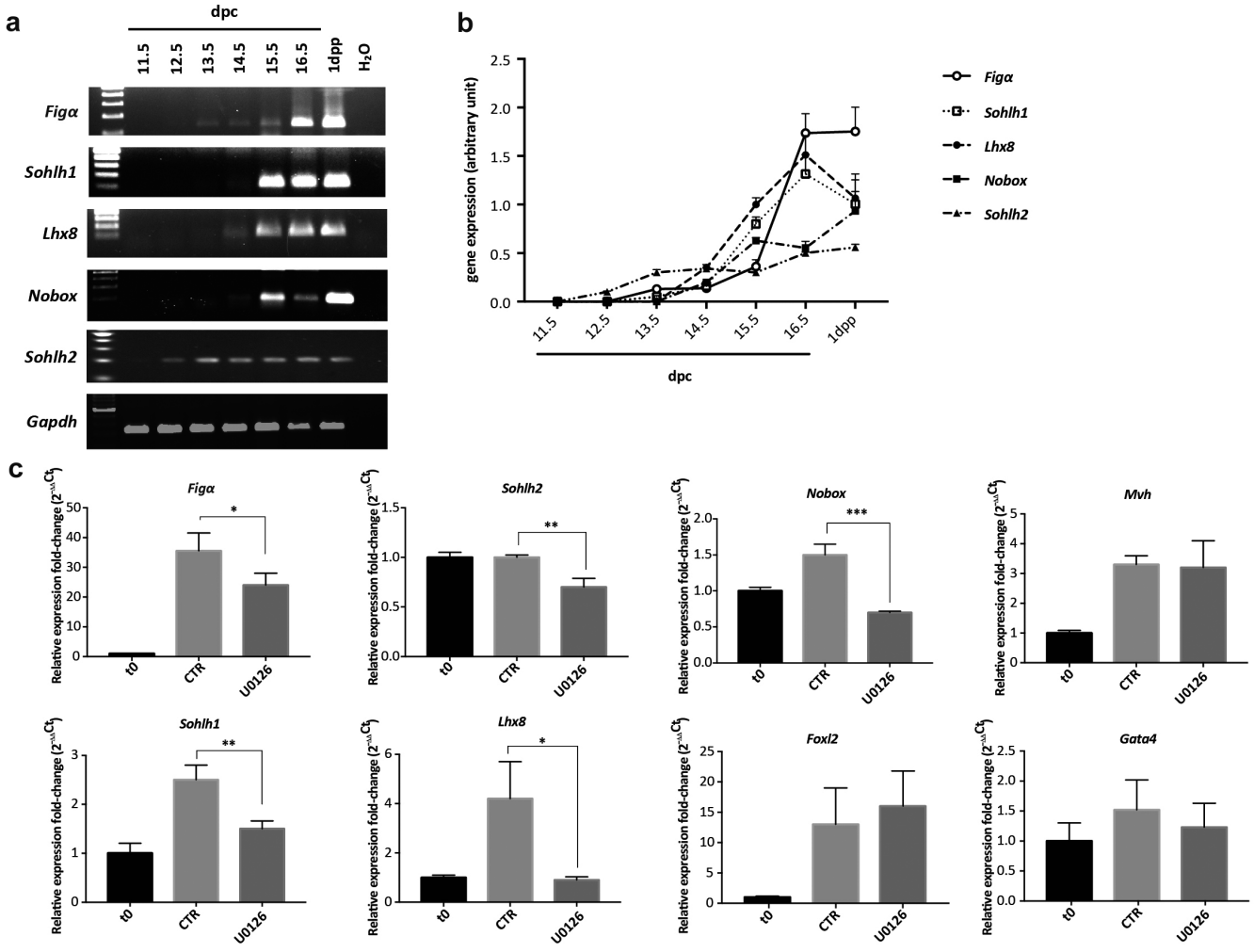

Fig. 3. Expression of germ cell-specific genes in gonadal ridges (GRs) and ovaries at different developmental ages. a: Representative RT-PCR analyses for the indicated genes performed in GRs (11.5 dpc) and ovaries at different ages from 12.5 dpc to 1 dpp. *Gapdh* was used as the general housekeeping gene, and *Mvh* was used as the germ cell-specific housekeeping gene. b: Graphic representation of the expression pattern of the genes resulting from the three experiments. Quantification of the bands from RT-PCR analysis was performed using ImageJ software (version 1.49v, Wayne Rasband, National Institutes of Health, USA) reflecting the amounts as a ratio of each band relative to the *Gapdh* lane (the means ± SEM are reported). c: Graphic representation of the qRT-PCR analyses showing the expression of the indicated genes relative to time zero (T0) in 12.5 dpc ovaries cultured for 48 h with or without 5 μM U0126. Note that the transcripts of all germ cell-specific genes except *Mvh* were significantly reduced in the presence of the inhibitor, namely those of *Nobox*, *Sohlh2*, and *Sohlh1*. The transcripts of the ovarian somatic cell genes *Foxl2* and *Gata4* were not significantly affected by U0126.

Inhibition of ERK1-2 activity in embryonic ovaries decreases oocyte number and impairs oocyte folliculogenesis in postnatal ovaries

To determine if the reduced expressions of the oocyte genes resulting from ERK1-2 activity inhibition reported above have consequences for correct oocyte differentiation and ovary development at subsequent stages, we set up a long-term *in vitro* culture system based on published protocol [28], allowing each ovary to develop to a prepuberal equivalent stage (around 10 dpp). For the first two days, 12.5 dpc ovaries were cultured in medium with or without 5 μM U0126 and subsequently for an additional 15 days without the inhibitor. The cultured ovaries were then analyzed for oocyte number and growth as well as the presence of follicles (Supplementary Figs. 2a and 2b: online only). We found that the ovaries cultured in the presence of U0126 contained a significantly reduced number of oocytes compared to the control ovaries (control: 95 ± 9, n = 11 *vs*. U0126: 49 ± 5, n = 8; Fig. 4a). Moreover, in both groups, > 90% of oocytes had a diameter between 20–50 μm and could be classified as growing oocytes. Finally, by examining histological sections, we observed that while nearly 90% of growing oocytes in the control ovaries were individually surrounded by follicular cells to form primary or secondary follicles, only about 50% of oocytes in the U0126-treated ovaries were enclosed by follicles; the rest remained in characteristic pre-follicular aggregates termed germ

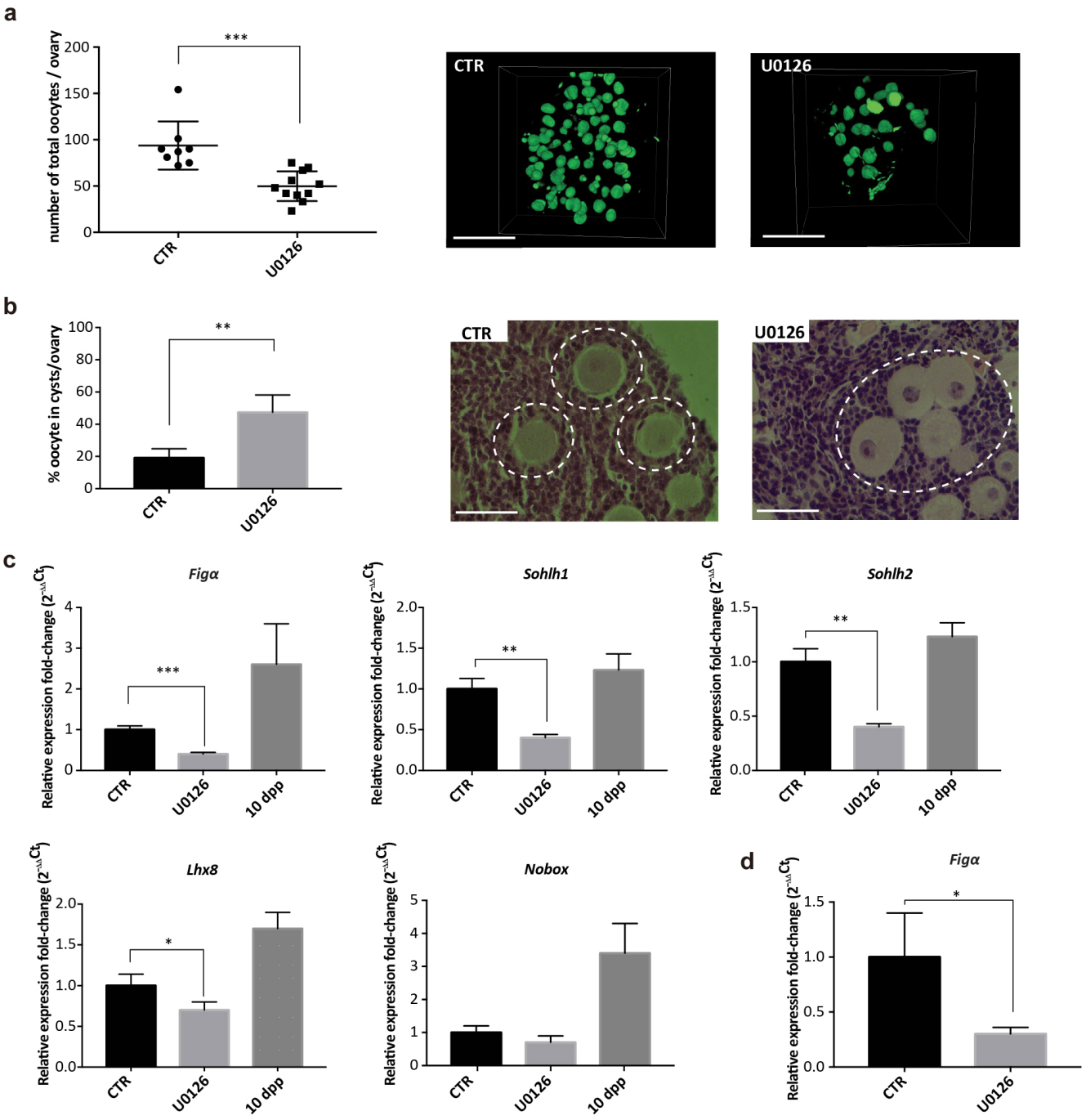

Fig. 4. Inhibition of ERK1-2 activity in embryonic ovaries: effects on oocyte number and folliculogenesis. a: Left – Number of oocytes scored in confocal sections of 12.5 dpc ovaries after 17 days of culture (ovaries were incubated in 5 µM U0126 for the first two days of culture only; see Supplementary Fig. 1). Right – Example of scored confocal sections. Scale bar: 200 µm. b: Left – Percent of oocytes in a cluster or single follicle after 17 days of culture as above. Right – Example of histological sections showing oocytes in a cluster or single follicle of the ovaries. Scale bar: 50 µM. c: Graphic representation of qRT-PCR analyses of the indicated genes resulting from three experiments (the means ± SEM are reported). All genes except *Nobox* showed reduced expression in the ovaries subjected to U0126 treatment (see above) in comparison to the CTR group, namely *Figα*, *Sohlh1*, and *Sohlh2*. d: Graphic representation of qRT-PCR analysis for *Figα* confirming a transcript reduction in oocytes isolated from U0126-treated ovaries in comparison to the CTR group.

cell cysts (Fig. 4b).

The qRT-PCR analysis results of the aforementioned oocyte-specific genes performed on ovaries at the end of culture are presented in Fig. 4c. Although the transcripts of all genes except *Nobox* were significantly decreased in *in vitro* cultured ovaries compared to their 10 dpp counterparts, U0126 treatment significantly reduced *Figα, Sohlh1*, and *Sohlh2* transcripts.

In order to verify that such reductions were not due to a lower oocyte number in the U0126-treated ovaries, qRT-PCR for *Figα*, the more significantly downregulated gene that controls the other oocyte-specific genes tested here [37], was performed in isolated oocytes obtained from the 17-day cultured ovaries. The results shown in Fig. 4d confirm a reduction in the transcript of this gene in oocytes from U0126 pre-treated ovaries compared to those of control ovaries.

Discussion

Studies in the last decade have revealed that ERKs play a pivotal role in regulating the mitotic and meiotic cell cycles as well as other crucial processes of cell biology, including migration and differentiation. In the present work, we analyzed the expression of p-ERK1-2 during the development of mouse PGCs (from 8.5 to 14.5 dpc) and used *in vitro* culture methods to investigate the functional role that these kinases may exert on crucial processes of PGC development.

Changes in activity and intracellular localization of ERK1-2 in PGCs

During migration and after arrival into the gonads, PGCs undergo several phenotypic, molecular, and epigenetic changes. Here, we showed that changes in ERK1-2 activities also accompany PGC development. While the presence of p-ERK1-2 in more than 50% of 9.5–10.5 dpc mouse PGCs has been reported by Takeuchi *et al*. [7], we found an additional transient decrease in the number of p-ERK1-2-positive PGCs at 11.5 dpc followed by a progressive increase at 13.5 dpc onward. The different percentages of ERK-positive cells likely reflect the dynamics of ERK activity at various developmental stages. Moreover, the action of several growth factors, particularly those of the FGF family [21], produced by the tissues crossed by the PGCs may also contribute to such variation (for a review, see [38, 39]).

ERK1-2 activity is required for proliferation of 8.5 but not 11.5 dpc PGCs

The findings that long-term [6] and short-term 24 h (this paper) proliferation of 8.5 dpc PGCs was significantly reduced in the presence of U0126 while that of 11.5 dpc PGCs was not indicate less stringent requirements for ERK activity during the more advanced stages of PGC expansion. In line with these results, Leitch *et al*. [40] reported a negative impact on EG cell colony formation from 8.5 dpc PGCs using a different inhibitor (PD0325901) in a defined culture system. Moreover, Choi *et al*. [41] showed that basic FGF stimulated the proliferation of chicken PGCs via MEK/ERK signaling. The apparent capability of 11.5 dpc PGCs to enter the S-phase even when the ERK pathway is inhibited is intriguing. It is possible that the G1/S transition does not require ERK1-2 activity and/or other kinases can substitute ERK function during mitosis in such cells. ERK activity is normally a key signal for the G1/S transition through the cyclin D/CDK checkpoint in G1 [42]. In this respect, the absence of a requirement for ERK activity for this transition in 11.5 dpc PGCs resembles that of mouse ES cells with an unorthodox cell cycle in which the G1 checkpoint does not appear to be operative, making the cycle relatively independent from the growth factor control [43]. In ES cells, loss of retinoblastoma (Rb) coupled with the constitutive activity of cyclinA/E-Cdk2 complexes may explain the lack of required ERK activity for proliferation [44]. In such contexts, ERK inhibition favors self-renewal, whereas activation exerts a pro-differentiation action ([45] and references herein). On the other hand, 11.5 dpc PGCs appear to possess more regulated control of the G1 phase [46] by various growth factors and compounds working through different signaling pathways (for a review, see [38, 39]). Therefore, rather than an unusual G1, it is more likely that the lack of required ERK activity for 11.5 dpc PGC expansion reflects the plurality of the proliferation stimuli and pathways operating on these cells at this stage (e.g., cAMP, KL/KIT, and BMP [47]).

ERK1-2 activity is necessary for PGC motility

Between 8.5 and 12.5 dpc, PGCs move from the wall of the yolk sac to the GRs. At least part of this movement is due to the activation of the motility machine and directional migration of the PGCs. Several studies have demonstrated that MAPKs play crucial roles in cell migration (for a review, see [48]). In particular, ERKs govern cell movement by myosin light chain kinase (MLCK), calpain, and focal adhesion kinase (FAK) phosphorylation. In previous studies, Takeuchi *et al*. [7] showed that the incubation of 9.5 and 10.5 dpc embryo slices with PGCs in FGF2- or FGF7-containing medium significantly increased the percentage of p-ERK1-2-positive PGCs and enhanced their movement. Using a cell directional migration assay, we found an approximate 30% reduction in PGC migration capability in the presence of U0126 [25]. In line with these results, we report that the frequency of PGCs displaying motility features onto cell monolayers after 24 h was significantly reduced by U0126, whereas the inhibitor did not affect PGC adhesion. This finding reinforces the notion that crucial processes of the complex molecular machine governing cell motility in PGCs could be dependent on ERKs. However, the possibility that STO cell monolayers are affected by U0126 cannot be excluded.

ERK1-2 activity is not required for the beginning of meiosis in female PGCs but necessary for correct meiotic prophase I progression

For the final stage of development, female PGCs enter meiosis in the ovary. Recent studies have shown that the initial choice of female or male identity in mice is governed by exposure to RA in the fetal gonad [32, 33]. These studies reported that although RA induces germ cells to enter meiosis in the ovary around 13.5 dpc, its degradation protects germ cells from entering meiosis in males at that time. Since we observed that the number of p-ERK-positive cells and p-ERK level increased in female PGCs concomitantly with their entry into meiosis, it made sense to investigate whether ERK activity was involved in such a crucial process. We found that while U0126 was unable to prevent the beginning of meiosis evaluated in oocyte cytospreads by the characteristic pattern of

chromosome SCP-3 immunostaining, the inhibitor did slow down meiotic progression. These results support the notion that in both vertebrate and invertebrates, the ERK/MAPK-signaling cascade regulates meiotic progression rather than initiation [1, 49–51]. The precise role of p-ERK1-2 in meiotic prophase I progression evidenced here remains to be investigated.

Inhibition of ERK1-2 activity in embryonic ovaries reduces oocyte-specific gene expression and impairs oocyte survival and folliculogenesis

Collectively, the results of the *in vitro* culture of 12.5 dpc ovaries in the presence of U0126 during a short window of development (between 12.5 and 14.5 dpc) indicate that the ERK1-2 activity increase registered during this period may be related to differentiation processes occurring in germ cells toward female identity that must be confirmed *in vivo*. In this regard, maintenance of the correct expression levels of genes, such as *Figα, Sohlh1, Sohlh2, Nobox,* and *Lhx8*, during this period appears crucial for oocyte survival as well as later follicle assembly and ERK1-2 activity critical to establishing the conditions for the correct expression of such genes in the oocytes. These results present ERK activation as a pathway involved in oocyte differentiation independent from entry into meiosis. Moreover, they support the role of ERK1-2 in PGC differentiation indirectly evidenced by the fact that, using PD0325901 in combination with a GSK-3 inhibitor plus LIF, both female and male mouse PGCs can be reprogrammed to pluripotent stem cells termed EG cells [14, 15]. What lies downstream of the ERK pathway and how it leads or sustains the transcriptional activation of oocyte differentiation genes will be the subject of future investigation.

Acknowledgments

Thanks to Graziano Bonelli for help with the figure and Gabriele Rossi for histological sections.

References

1. **Fan HY, Sun QY.** Involvement of mitogen-activated protein kinase cascade during oocyte maturation and fertilization in mammals. *Biol Reprod* 2004; **70**: 535–547. [Medline] [CrossRef]
2. **Arur S.** Signaling-Mediated Regulation of Meiotic Prophase I and Transition During Oogenesis. *Results Probl Cell Differ* 2017; **59**: 101–123. [Medline] [CrossRef]
3. **Pesce M, Klinger FG, De Felici M.** Derivation in culture of primordial germ cells from cells of the mouse epiblast: phenotypic induction and growth control by Bmp4 signalling. *Mech Dev* 2002; **112**: 15–24. [Medline] [CrossRef]
4. **Aubin J, Davy A, Soriano P.** In vivo convergence of BMP and MAPK signaling pathways: impact of differential Smad1 phosphorylation on development and homeostasis. *Genes Dev* 2004; **18**: 1482–1494. [Medline] [CrossRef]
5. **Grabole N, Tischler J, Hackett JA, Kim S, Tang F, Leitch HG, Magnúsdóttir E, Surani MA.** Prdm14 promotes germline fate and naive pluripotency by repressing FGF signalling and DNA methylation. *EMBO Rep* 2013; **14**: 629–637. [Medline] [CrossRef]
6. **De Miguel MP, Cheng L, Holland EC, Federspiel MJ, Donovan PJ.** Dissection of the c-Kit signaling pathway in mouse primordial germ cells by retroviral-mediated gene transfer. *Proc Natl Acad Sci USA* 2002; **99**: 10458–10463. [Medline] [CrossRef]
7. **Takeuchi Y, Molyneaux K, Runyan C, Schaible K, Wylie C.** The roles of FGF signaling in germ cell migration in the mouse. *Development* 2005; **132**: 5399–5409. [Medline] [CrossRef]
8. **Okamura D, Mochizuki K, Taniguchi H, Tokitake Y, Ikeda M, Yamada Y, Tournier C, Yamaguchi S, Tada T, Schöler HR, Matsui Y.** REST and its downstream molecule Mek5 regulate survival of primordial germ cells. *Dev Biol* 2012; **372**: 190–202. [Medline] [CrossRef]
9. **Chen H, Palmer JS, Thiagarajan RD, Dinger ME, Lesieur E, Chiu H, Schulz A, Spiller C, Grimmond SM, Little MH, Koopman P, Wilhelm D.** Identification of novel markers of mouse fetal ovary development. *PLoS One* 2012; **7**: e41683. [Medline] [CrossRef]
10. **Sakashita A, Kawabata Y, Jincho Y, Tajima S, Kumamoto S, Kobayashi H, Matsui Y, Kono T.** Sex specification and heterogeneity of primordial germ cells in mice. *PLoS One* 2015; **10**: e0144836. [Medline] [CrossRef]
11. **Ulu F, Kim SM, Yokoyama T, Yamazaki Y.** Dose-dependent functions of fibroblast growth factor 9 regulate the fate of murine XY primordial germ cells. *Biol Reprod* 2017; **96**: 122–133. [Medline] [CrossRef]
12. **Ewen K, Jackson A, Wilhelm D, Koopman P.** A male-specific role for p38 mitogen-activated protein kinase in germ cell sex differentiation in mice. *Biol Reprod* 2010; **83**: 1005–1014. [Medline] [CrossRef]
13. **Wu Q, Fukuda K, Weinstein M, Graff JM, Saga Y.** SMAD2 and p38 signaling pathways act in concert to determine XY primordial germ cell fate in mice. *Development* 2015; **142**: 575–586. [Medline] [CrossRef]
14. **Leitch HG, Blair K, Mansfield W, Ayetey H, Humphreys P, Nichols J, Surani MA, Smith A.** Embryonic germ cells from mice and rats exhibit properties consistent with a generic pluripotent ground state. *Development* 2010; **137**: 2279–2287. [Medline] [CrossRef]
15. **Nagamatsu G, Kosaka T, Saito S, Takubo K, Akiyama H, Sudo T, Horimoto K, Oya M, Suda T.** Tracing the conversion process from primordial germ cells to pluripotent stem cells in mice. *Biol Reprod* 2012; **86**: 182. [Medline] [CrossRef]
16. **Kimura T, Kaga Y, Ohta H, Odamoto M, Sekita Y, Li K, Yamano N, Fujikawa K, Isotani A, Sasaki N, Toyoda M, Hayashi K, Okabe M, Shinohara T, Saitou M, Nakano T.** Induction of primordial germ cell-like cells from mouse embryonic stem cells by ERK signal inhibition. *Stem Cells* 2014; **32**: 2668–2678. [Medline] [CrossRef]
17. **Irie N, Weinberger L, Tang WW, Kobayashi T, Viukov S, Manor YS, Dietmann S, Hanna JH, Surani MA.** SOX17 is a critical specifier of human primordial germ cell fate. *Cell* 2015; **160**: 253–268. [Medline] [CrossRef]
18. **Mitsunaga S, Odajima J, Yawata S, Shioda K, Owa C, Isselbacher KJ, Hanna JH, Shioda T.** Relevance of iPSC-derived human PGC-like cells at the surface of embryoid bodies to prechemotaxis migrating PGCs. *Proc Natl Acad Sci USA* 2017; **114**: E9913–E9922. [Medline] [CrossRef]
19. **Cairns LA, Moroni E, Levantini E, Giorgetti A, Klinger FG, Ronzoni S, Tatangelo L, Tiveron C, De Felici M, Dolci S, Magli MC, Giglioni B, Ottolenghi S.** Kit regulatory elements required for expression in developing hematopoietic and germ cell lineages. *Blood* 2003; **102**: 3954–3962. [Medline] [CrossRef]
20. **De Felici M, Pesce M, Giustiniani Q, Di Carlo A.** In vitro adhesiveness of mouse primordial germ cells to cellular and extracellular matrix component substrata. *Microsc Res Tech* 1998; **43**: 258–264. [Medline] [CrossRef]
21. **Farini D, Scaldaferri ML, Iona S, La Sala G, De Felici M.** Growth factors sustain primordial germ cell survival, proliferation and entering into meiosis in the absence of somatic cells. *Dev Biol* 2005; **285**: 49–56. [Medline] [CrossRef]
22. **De Felici M, McLaren A.** Isolation of mouse primordial germ cells. *Exp Cell Res* 1982; **142**: 476–482. [Medline] [CrossRef]
23. **Pesce M, Di Carlo A, De Felici M.** The c-kit receptor is involved in the adhesion of mouse primordial germ cells to somatic cells in culture. *Mech Dev* 1997; **68**: 37–44. [Medline] [CrossRef]
24. **Donovan PJ, Stott D, Cairns LA, Heasman J, Wylie CC.** Migratory and postmigratory mouse primordial germ cells behave differently in culture. *Cell* 1986; **44**: 831–838. [Medline] [CrossRef]
25. **Farini D, La Sala G, Tedesco M, De Felici M.** Chemoattractant action and molecular signaling pathways of Kit ligand on mouse primordial germ cells. *Dev Biol* 2007; **306**: 572–583. [Medline] [CrossRef]
26. **Pesce M, De Felici M.** Purification of mouse primordial germ cells by MiniMACS magnetic separation system. *Dev Biol* 1995; **170**: 722–725. [Medline] [CrossRef]
27. **Chuma S, Nakatsuji N.** Autonomous transition into meiosis of mouse fetal germ cells in vitro and its inhibition by gp130-mediated signaling. *Dev Biol* 2001; **229**: 468–479. [Medline] [CrossRef]
28. **Morohaku K, Hirao Y, Obata Y.** Development of fertile mouse oocytes from mitotic germ cells in vitro. *Nat Protoc* 2017; **12**: 1817–1829. [Medline] [CrossRef]
29. **De Felici M, Dolci S, Pesce M.** Proliferation of mouse primordial germ cells in vitro: a key role for cAMP. *Dev Biol* 1993; **157**: 277–280. [Medline] [CrossRef]
30. **Dolci S, Pesce M, De Felici M.** Combined action of stem cell factor, leukemia inhibitory factor, and cAMP on in vitro proliferation of mouse primordial germ cells. *Mol Reprod Dev* 1993; **35**: 134–139. [Medline] [CrossRef]
31. **Barrios F, Filipponi D, Pellegrini M, Paronetto MP, Di Siena S, Geremia R, Rossi P, De Felici M, Jannini EA, Dolci S.** Opposing effects of retinoic acid and FGF9 on Nanos2 expression and meiotic entry of mouse germ cells. *J Cell Sci* 2010; **123**: 871–880. [Medline] [CrossRef]
32. **Bowles J, Knight D, Smith C, Wilhelm D, Richman J, Mamiya S, Yashiro K,**

Chawengsaksophak K, Wilson MJ, Rossant J, Hamada H, Koopman P. Retinoid signaling determines germ cell fate in mice. *Science* 2006; **312**: 596–600. [Medline] [CrossRef]

33. **Koubova J, Menke DB, Zhou Q, Capel B, Griswold MD, Page DC.** Retinoic acid regulates sex-specific timing of meiotic initiation in mice. *Proc Natl Acad Sci USA* 2006; **103**: 2474–2479. [Medline] [CrossRef]
34. **Kato T, Ohtani-Kaneko R, Ono K, Okado N, Shiga T.** Developmental regulation of activated ERK expression in the spinal cord and dorsal root ganglion of the chick embryo. *Neurosci Res* 2005; **52**: 11–19. [Medline] [CrossRef]
35. **Shin Y-H, Ren Y, Suzuki H, Golnoski KJ, Ahn HW, Mico V, Rajkovic A.** Transcription factors SOHLH1 and SOHLH2 coordinate oocyte differentiation without affecting meiosis I. *J Clin Invest* 2017; **127**: 2106–2117. [Medline] [CrossRef]
36. **Dokshin GA, Baltus AE, Eppig JJ, Page DC.** Oocyte differentiation is genetically dissociable from meiosis in mice. *Nat Genet* 2013; **45**: 877–883. [Medline] [CrossRef]
37. **Bayne RAL, Martins da Silva SJ, Anderson RA.** Increased expression of the FIGLA transcription factor is associated with primordial follicle formation in the human fetal ovary. *Mol Hum Reprod* 2004; **10**: 373–381. [Medline] [CrossRef]
38. **De Felici M.** Regulation of primordial germ cell development in the mouse. *Int J Dev Biol* 2000; **44**: 575–580. [Medline]
39. **De Felici M, Farini D, Dolci S.** In or out stemness: comparing growth factor signalling in mouse embryonic stem cells and primordial germ cells. *Curr Stem Cell Res Ther* 2009; **4**: 87–97. [Medline] [CrossRef]
40. **Leitch HG, Nichols J, Humphreys P, Mulas C, Martello G, Lee C, Jones K, Surani MA, Smith A.** Rebuilding pluripotency from primordial germ cells. *Stem Cell Reports* 2013; **1**: 66–78. [Medline] [CrossRef]
41. **Choi JW, Kim S, Kim TM, Kim YM, Seo HW, Park TS, Jeong J-W, Song G, Han JY.** Basic fibroblast growth factor activates MEK/ERK cell signaling pathway and stimulates the proliferation of chicken primordial germ cells. *PLoS One* 2010; **5**: e12968. [Medline] [CrossRef]
42. **Roovers K, Assoian RK.** Integrating the MAP kinase signal into the G1 phase cell cycle machinery. *BioEssays* 2000; **22**: 818–826. [Medline] [CrossRef]
43. **Savatier P, Lapillonne H, van Grunsven LA, Rudkin BB, Samarut J.** Withdrawal of differentiation inhibitory activity/leukemia inhibitory factor up-regulates D-type cyclins and cyclin-dependent kinase inhibitors in mouse embryonic stem cells. *Oncogene* 1996; **12**: 309–322. [Medline]
44. **D'Abaco GM, Hooper S, Paterson H, Marshall CJ.** Loss of Rb overrides the requirement for ERK activity for cell proliferation. *J Cell Sci* 2002; **115**: 4607–4616. [Medline] [CrossRef]
45. **Binétruy B, Heasley L, Bost F, Caron L, Aouadi M.** Concise review: regulation of embryonic stem cell lineage commitment by mitogen-activated protein kinases. *Stem Cells* 2007; **25**: 1090–1095. [Medline] [CrossRef]
46. **Sorrentino E, Nazzicone V, Farini D, Campagnolo L, De Felici M.** Comparative transcript profiles of cell cycle-related genes in mouse primordial germ cells, embryonic stem cells and embryonic germ cells. *Gene Expr Patterns* 2007; **7**: 714–721. [Medline] [CrossRef]
47. **De Felici M, Farini D.** The control of cell cycle in mouse primordial germ cells: old and new players. *Curr Pharm Des* 2012; **18**: 233–244. [Medline] [CrossRef]
48. **Huang C, Jacobson K, Schaller MD.** MAP kinases and cell migration. *J Cell Sci* 2004; **117**: 4619–4628. [Medline] [CrossRef]
49. **Church DL, Guan KL, Lambie EJ.** Three genes of the MAP kinase cascade, mek-2, mpk-1/sur-1 and let-60 ras, are required for meiotic cell cycle progression in Caenorhabditis elegans. *Development* 1995; **121**: 2525–2535. [Medline]
50. **Lee MH, Ohmachi M, Arur S, Nayak S, Francis R, Church D, Lambie E, Schedl T.** Multiple functions and dynamic activation of MPK-1 extracellular signal-regulated kinase signaling in Caenorhabditis elegans germline development. *Genetics* 2007; **177**: 2039–2062. [Medline] [CrossRef]
51. **Nadarajan S, Mohideen F, Tzur YB, Ferrandiz N, Crawley O, Montoya A, Faull P, Snijders AP, Cutillas PR, Jambhekar A, Blower MD, Martinez-Perez E, Harper JW, Colaiacovo MP.** The MAP kinase pathway coordinates crossover designation with disassembly of synaptonemal complex proteins during meiosis. *eLife* 2016; **5**: e12039. [Medline] [CrossRef]